

AN ANALYTICAL METHOD FOR STUDYING THE STRESS-STRAIN RELATIONS OF BULK METALLIC GLASS MATRIX COMPOSITES UNDER TENSION

Yunpeng Jiang

State Key Laboratory of Mechanics and Control of Mechanical, Nanjing University of Aeronautics and Astronautics, Nanjing 210016, China
E-mail: yppjiang@nuaa.edu.cn

Received 14 July 2016; accepted 15 September 2016

ABSTRACT

In this contribution, an analytical model was formulated to predict the tensile stress-strain relations of bulk metallic glass matrix composites (BMGCs) based on Weng's theoretical frame for dual-ductile composites. For in-situ BMGCs, BMG matrix also exhibits the elastic-plastic deform response as well as the dendrite phases during the stretching. The shear bands are regarded as Mode-I cracks, and whereby the strain-softening stage in the stress-strain curves can be well reflected. Furthermore, multi-particle representative volume element based FEM modelling was employed to clearly explain the failure mechanisms in BMGCs as a necessary complement. The predictions are in reasonable agreement with the experimental results. The presented analytical method will shed some light on optimizing the microstructures, and is of convenience in the engineering applications.

Keywords: Bulk metallic glass composites (BMGs); Shear band; Microstructure; Stress-strain relations; Analytical model

1. INTRODUCTION

Bulk metallic glasses (BMGs) have many unique properties, e.g., exceptionally high strength, large elastic limit, high hardness, good corrosion resistance and reduced sliding friction etc. and are, therefore, regarded as potential candidates for engineering materials [1-2]. However, their structural application is so far severely stymied by their limited intrinsic plasticity that is confined to narrow regions near dilute shear bands at room temperature [3]. Generally, introducing crystalline second phase precipitates or particles can effectively generate multiple shear-banding and impede rapid shear band propagation [4]. Therefore, BMG composites could effectively circumvent the poor damage tolerance of BMGs. Up to date, the drastic changes in the production method and material form have also resulted in significant extension of application fields of glassy alloys.

Despite the fact that a large number of investigations have already been performed and many qualitative conclusions were reached, we, however, are far away from a complete and thorough understanding of the fundamental synergic mechanisms governing the compatible deformations between the soft and ductile second phase reinforcements and the hard and brittle matrix in BMG composites. Analytical models are more efficient than those numerical methods, but lag far behind the experiments and simulations. Based on the principle of thermodynamics and free energy, Marandi et al. [5] developed an elastic-viscoplastic, three-dimensional, finite deformation constitutive model to describe the large deformation behaviour of BMG composite, but their model is fairly complicated and short of the micromechanics significance. Marandi et al. [6] established an elastic-viscoplastic, three-dimensional, finite deformation constitutive model to describe the behaviour of La-based in-situ BMG composite (*In-situ*

composites are multiphase materials where the reinforcing phase is synthesized within the matrix during composite fabrication), within the super-cooled liquid region, at ambient pressure and a range of strain rates. Yang et al. [7] developed a constitutive model of BMG plasticity which accounts for finite deformation kinematics, the kinetics of free volume, strain hardening, thermal softening, rate-dependency and non-Newtonian viscosity. The model has been validated against uniaxial compression test data; and against plate bending experiments. Qiao et al. [8] firstly gave a mathematical model to elucidate the work-hardening behaviour of ductile dendrites and softening of the amorphous matrix, and could fatherly simulate the tensile response of BMG composites, yet the interaction between two phases was not well considered. Only quantitative relations can further greatly improve the ductility/toughness of BMGs via efficiently tailoring the microstructures in an optimized manner. It is impeding to establish quantitative relations between microstructure parameters and material properties at the mesoscopic scale. Recently, Sun et al. [9] improved their previous micromechanics model to better predict the tensile behaviours of in-situ BMG composites based the in-situ measured data by the nano-indentation test.

Although a quantity of theoretical studies have been performed and provided insight into the mechanical behaviours of BMG composites, an explicit micromechanics model to explain and describe their intriguing experimental results is still lacking. This paper develops an analytical model to describe the failure behaviour of BMG composites by introducing stochastic approaches and accounting for the roles of shear banding in the plastic deformation. A composite model is used to calculate the stress-strain responses, which are compared with the experiments that

are available in the published literatures, followed by the numerical analysis and discussion on the microstructure parameters.

2. MICROMECHANICAL COMPOSITE MODEL

BMGs exhibit brittle under unconstrained testing conditions, such as uniaxial compression, tension and bending. However, they also present plastic deformation ability to a certain extent under multi-axial stress state. Many previous experiments [10-11] have already confirmed this conclusion, and correspondingly the mechanical behaviours under the multi-axial stress state are largely different from those in the uniaxial stress state for BMGs. Therefore, the BMG matrix is also regarded as elastic-plastic phase that is similar to the ductile particles.

For a two-phase composite system, the particle phase will be referred as phase 1 and matrix as phase 0 throughout the paper, and those of the composite are denoted by symbols without any script. All the tensors and vectors are written in boldface letters. The volume fractions of the particles and matrix are denoted by f_1 and f_0 , respectively, and satisfy the relation $f_1 + f_0 = 1$. The Ludwik equation is adopted for the constituents in terms of von Mises' effective stress and plastic strain

$$\sigma_{eq}^{(r)} = \sigma_y^{(r)} + h_r (\varepsilon_{eq}^{p(r)})^{n_r} \quad (1)$$

in which $\sigma_{eq}^{(r)} = (3\sigma_{ij}^{(r)}\sigma_{ij}^{(r)}/2)^{1/2}$, $\varepsilon_{eq}^{p(r)} = (2\varepsilon_{ij}^{p(r)}\varepsilon_{ij}^{p(r)}/3)^{1/2}$ and then in terms of the effective strain the secant Young's modulus and secant Poisson ratio of the r -th phase is written as:

$$E_r^S = \frac{1}{\frac{1}{E_r} + \frac{\varepsilon_{eq}^{p(r)}}{\sigma_y^{(r)} + h_r (\varepsilon_{eq}^{p(r)})^{n_r}}}, \quad \nu_r^S = \frac{1}{2} - \left(\frac{1}{2} - \nu_r\right) \frac{E_r^S}{E_r} \quad (2)$$

Correspondingly, the secant bulk and shear moduli of the r -th phase are written as follows to meet the isotropic relations,

$$\kappa_r^S = \frac{E_r^S}{3(1-2\nu_r^S)}, \quad \mu_r^S = \frac{E_r^S}{2(1+\nu_r^S)} \quad (3)$$

Fig. 1 shows the schematic diagram showing the damage model that is adopted for describing the mechanical behaviours of BMG composites. At an arbitrary material point, the composite system constitutes of ductile particles, shear bands and BMG matrix. Suppose that the composite is subject to a uniform strain boundary displacement of $\bar{\varepsilon}$, based on the composite model developed by Weng [12], and later modified by Zhu [13], the constitutive relation between the hydrostatic and deviatoric strains of composite obeys:

$$\begin{aligned} \bar{\sigma}_{kk} &= 3\kappa_0 [1 + f_1(A_1 - A_0)] \bar{\varepsilon}_{kk}, \\ \bar{\sigma}_{ij}' &= 2\mu_0^S \left[\left(1 + \frac{f_1 B_1}{\beta_0^S} \right) \bar{\varepsilon}_{ij}' - \frac{f_1 B_0}{\beta_0^S} \varepsilon_{ij}^{p(1)} \right] \end{aligned} \quad (4)$$

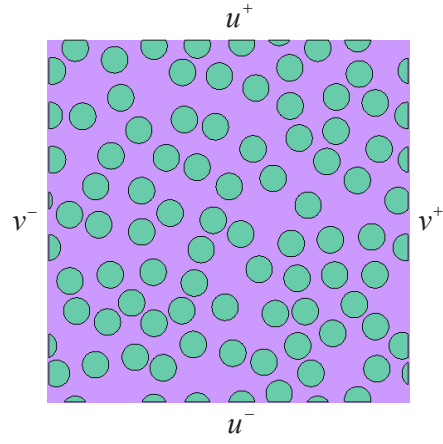


Fig. 1: Plane strain computational multi-particle cell model and the corresponding boundary conditions.

Here:

$$A_0 = \frac{\kappa_0}{f_0 \alpha_0^S (\kappa_1 - \kappa_0) + \kappa_0}, \quad A_1 = \frac{\kappa_1}{f_0 \alpha_0^S (\kappa_1 - \kappa_0) + \kappa_0} \quad (5)$$

$$B_0 = \frac{\beta_0^S \mu_1}{f_0 \beta_0^S (\mu_1 - \mu_0^S) + \mu_0^S}, \quad B_1 = \frac{\beta_0^S (\mu_1 - \mu_0^S)}{f_0 \beta_0^S (\mu_1 - \mu_0^S) + \mu_0^S} \quad (6)$$

In which, the α_0^S and β_0^S are the components of Eshelby's tensor for spherical inclusions following $\mathbf{S}_0^S = (\alpha_0^S, \beta_0^S)$, where:

$$\alpha_0^S = (1 + \nu_0^S) / 3(1 - \nu_0^S), \quad \beta_0^S = 2(4 - 5\nu_0^S) / 15(1 - \nu_0^S) \quad (7)$$

3. SHEAR BANDING EFFECT

Experimental observations show that the shear bands would eventually evolve into micro-cracks with the local deformation increasing, and thus shear bands are equivalent to micro-cracks. Because the micro-cracks generated during the shear banding are supposed to be randomly dispersed, the corresponding effective moduli are as follows [14]

$$\frac{E}{E_0} = \left[1 + \frac{16(1-\nu_0^2)(1-3\nu_0/10)}{9(1-\nu_0/2)} \rho \right]^{-1} \quad (8)$$

$$\frac{G}{G_0} = \left[1 + \frac{16(1-\nu_0)(1-\nu_0/5)}{9(1-\nu_0/2)} \rho \right]^{-1} \quad (9)$$

$$\frac{\nu}{\nu_0} = \frac{E}{E_0} \left[1 + \frac{8(1-\nu_0^2)}{45(1-\nu_0/2)} \rho \right] \quad (10)$$

where ρ denotes the crack density in the representative volume element. For the ductile materials, the failure criterion based on statistical probability is associated with strain. The strain-based Weibull distribution function is addressed to characterize the micro-crack-induced fracture as follows:

$$P(\varepsilon_p) = 1 - \exp \left[- \left(\frac{\varepsilon_p}{\varepsilon_0} \right)^m \right] \quad (11)$$

where ε_p is the plastic strain and ε_0 is the reference strain. Then, the density of micro-cracks in the BMG composites can be rewritten as:

$$\rho = \rho_0 \cdot P(\varepsilon_p) = \rho_0 \cdot \left\{ 1 - \exp \left[- \left(\frac{\varepsilon_p}{\varepsilon_0} \right)^m \right] \right\} \quad (12)$$

here, ρ_0 denotes the saturate density of micro-cracks, and m is the Weibull modulus.

4. FEM SIMULATION

Generally, particles are randomly distributed in the BMG matrix, and therefore, FEM modelling is to be performed to obtain a clear snapshot of the micro-deformations process under tension as a necessary compliment to the above model. Since the main features of the shear banding mechanism are better revealed in two-dimensional plane-strain calculations, and thus two dimensional models are adopted in the whole simulations. Multi-particle computation model as shown in Fig. 1 is meshed through 2D eight-node plain strain elements CPE4R, here quadrilateral, isoparametric elements are employed in the discretization, and reduced integration is used. here 80 particles are introduced in the composite system with particle volume fraction 40%. Periodic boundary conditions are applied through the multi-point boundary method ‘equation’ in the ABAQUS code [15]. The periodical boundary conditions on the corresponding nodes at the surfaces are imposed by:

$$u^+ - u^- = \lambda_1 \quad (13)$$

$$v^+ - v^- = \lambda_2 \quad (14)$$

where λ_1 and λ_2 are the applied displacement, the superscripts ‘ \pm ’ denote the two opposite surfaces along a certain direction, and u and v denote the stretched displacements along the x and y directions, respectively. According to the essential damage features of BMG, the shear damage criterion is employed in characterizing the shear banding evolution in BMG composites. The stiffness degradation in shear damage process is monitored to capturing the progressive shear banding.

5. RESULTS AND DISCUSSION

5.1 Comparison with experiment on stress–strain relations

Two set of experimental results are used to verify the correctness of the developed model. Fig. 2 shows the first comparisons between the numerical prediction and experiments for BMG composite with dendrite volume fraction of $f_p=43\%$ [16], where two sets of experimental results are listed. Here, $E_0=132$ GPa, $\nu_0=0.3$, $\sigma_0=1860$ MPa, $h_0=2.0 \times 10^5$ MPa, $n_0=2$ and $E1=86$ GPa, $\nu_1=0.27$, $\sigma_1=480$ MPa, $h_1=180$ MPa, $n_1=0.15$. Fig. 3 shows the second comparisons of stress–strain relations between the theoretical prediction and experiments for BMG composite with various dendrite volume fractions [17] with 33%, 49% and 58%.

Where, $E_1=78.3$ GPa, $\nu_1=0.375$, $\sigma_1=410$ MPa, $h_1=125$ MPa, $n_1=0.13$, $E_0=89.7$ GPa, $\nu_0=0.355$, $\sigma_0=1737$ MPa, $h_0=1.2 \times 10^5$ MPa and $n_0=2$. The present predictions are in agreement with the corresponding experimental results, which confirm the accuracy of the developed simulations. The proposed computational micromechanics model appears to be capable of capturing the constitutive behaviours of BMG composites.

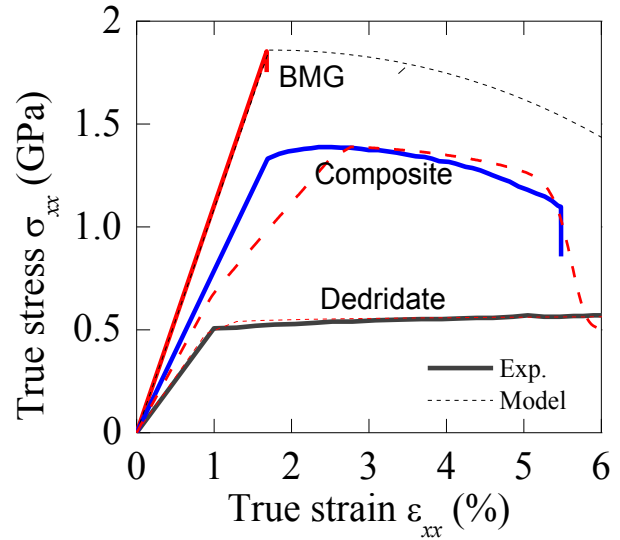


Fig. 2: Comparisons between the numerical prediction and experiments for BMG composite with dendrite volume fraction of $f_p=43\%$ [1], where two sets of experimental results are listed.

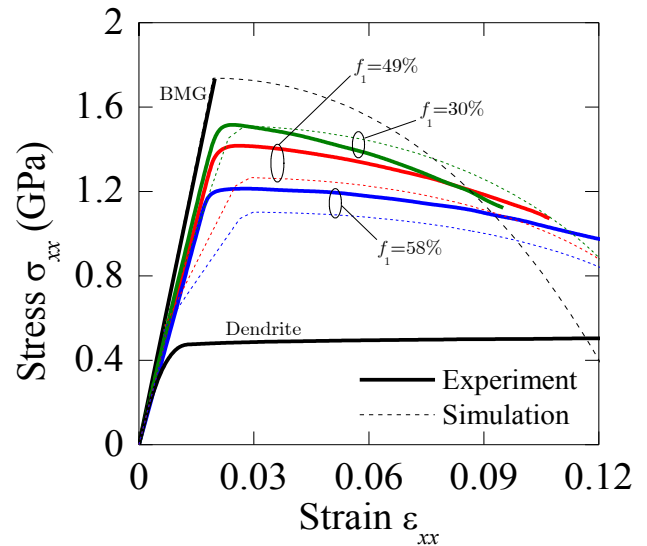


Fig. 3: Comparisons of stress–strain relations between the theoretical prediction and experiments for BMG composite with various dendrite volume fractions [3].

5.2 Effect of Weibull modulus m and reference strain ε_0

To analyse the role of the Weibull modulus and reference strain on the mechanical performance, the stress–strain response with different ε_0 is predicted and plotted in Fig. 4, which showed that the uniform elongation decreases with increasing referenced crack density. The variation of the elongation becomes remarkable as the reference strain is

less than 0.1, while the elongation decreases asymptotically as the reference strain increases to a large value. Furthermore, Fig. 5 shows the calculated stress–strain relations as the Weibull modulus m increase from 3 to 28 with the constant reference strain 0.1. As the volume fraction of constituents is unchanged, these results reveal that the ductility decreases with decreasing Weibull modulus m . This is consistent with the definition of the Weibull modulus. In the statistical analysis, Weibull modulus should be an important parameter in all the analytical models, and greatly influences the deformation responses of the materials. The specific value of Weibull modulus relies on many microstructure parameters, such as particle size, morphology, dispersion state, interface properties and so on. The relevant studies and the detailed roles in the damage process have been also analysed [18-21]. Numerical results show that increasing both ϵ_0 and m all remarkably improve the plastic deformability of BMG composites.

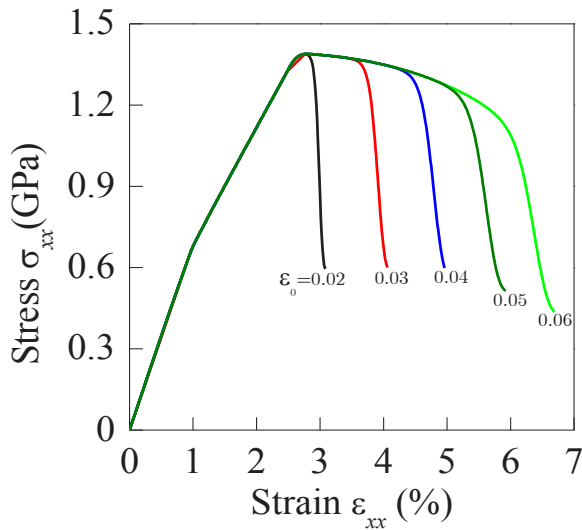


Fig. 4: Stress–strain response of BMG composites with different reference strain ϵ_0 .

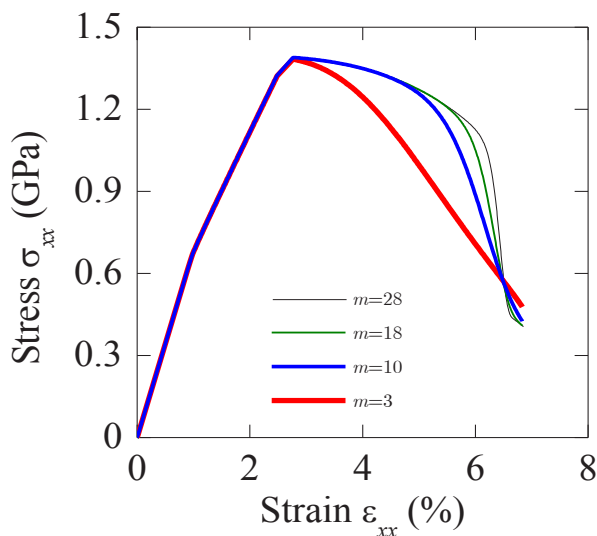


Fig. 5: Stress–strain response of BMG composites with different Weibull modulus m .

5.3 Comparison between FEM simulation and analytical model

Besides the preceding predictions from micromechanics, FEM modelling is performed to illustrate the shear banding propagation as a necessary complement. Fig. 6 shows the comparison between the stress–strain curves predicted by the developed analytical model and FEM simulation, and the snapshot of shear banding at the final failure is also attached. It should be noticed that the shear band initiates at the interface between particles and BMG matrix due to the stress concentration effect. Correspondingly, the shear bands will interact with each other, and form an intersecting network. It should be noted that ductile particles within shear band domains deformed seriously, and thus experience a phase transition in the actual composites. This is also confirmed by some experimental observations. These interplays among them would undoubtedly increase the plastic deformation zone, and thus remarkably improve the tensile ductility of composite system.

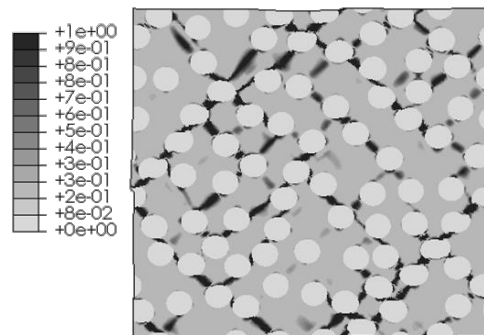
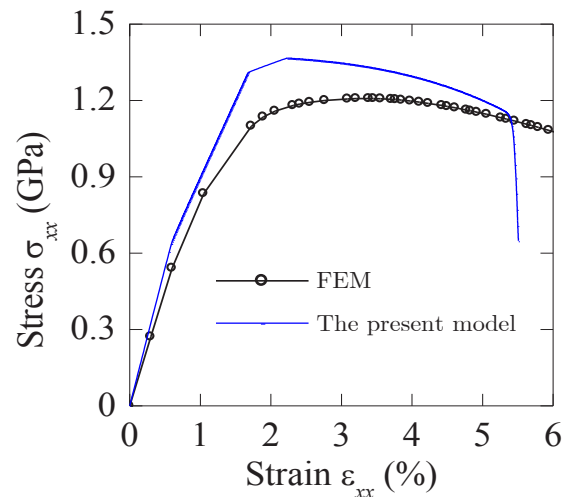


Fig. 6: Comparison between the stress–strain curves predicted by the present analytical model and FEM simulation, and the contour of shear banding at the final failure.

6. CONCLUSIONS

A simple analytical model was developed for predicting the tensile stress–strain relations of BMG composites with the help of Weng’s theoretical frame for dual-ductile composites. Here, BMG matrix exhibits the elastic–plastic deform response as well as the dendrite phases during the deformation, and furthermore the shear bands are regarded as Mode-I cracks by which the strain-softening stage in

the stress-strain curves can be well reflected. The present model could catch the main features of the mechanical response of BMG composites, and the effect of some coefficients on the stress-strain curves is also discussed.

ACKNOWLEDGEMENTS

This work was supported by the Fundamental Research Funds for the Central Universities (No.B11020079), Jiangsu Provincial Natural Science Foundation (No. BK2012407), National Natural Science Foundation of China (11202064) and Program for New Century Excellent Talents in University.

References:

1. W.H. Wang. *Prog Mater Sci* 57(2012): 487–656.
2. J.W. Qiao, H.L. Jia and P.K. Liaw. *Mater Sci Eng R* 100 (2016): 1–69.
3. G. He, J. Eckert, W. Löser and L. Schultz. *Nat Mater* 2(2003): 33–37.
4. A.L. Greer, Y.Q. Cheng and E. Ma. *Mater Sci Eng R* 74(2013): 71–132.
5. K. Marandi and V.P.W. Shim. *Continuum Mech Thermodyn* 26(2014): 321–341.
6. K. Marandi, P. Thamburaja and V.P.W. Shim. *Mech Mater* 75(2014): 151–164.
7. Q. Yang, A. Mota and M. Ortiz. *Comput Mech* 37(2006): 194–204.
8. J.W. Qiao, T. Zhang, F.Q. Yang, P.K. Liaw, S. Pauly and B.S. Xu. *Sci Rep* 3(2013): Doi: 10.1038/srep02816.
9. X.H. Sun, J.W. Qiao, Z.M. Jiao, Z.H. Wang, H.J. Yang and B.S. Xu. *Sci Rep* 5(2015): Doi: 10.1038/srep13964.
10. R. D. Conner, W. L. Johnson, N. E. Paton and W. D. Nix. *J Appl Phys* 94(2003): 904–911
11. C. Su and L. Anand. *Acta Mater* 54(2006): 179–189.
12. G.J. Weng. *J Mech Phys Solid* 38(1990): 419–441.
13. L.L. Zhu and J. Lu. *Int J Plasticity* 30(2012): 166–184.
14. M. Kachanov. *Adv Appl Mech* 30(1994): 259–445.
15. ABAQUS theory manual, (HKS inc., 2010), pp. 510.
16. J.W. Qiao, A.C. Sun, E.W. Huang, Y. Zhang, P.K. Liaw and C.P. Chuang. *Acta Mater* 59(2011): 4126–4137.
17. D.C. Hofmann, J.Y. Suh, Wiest A, et al. *Nature* 451(2008): 1085–1089.
18. M. Sutcu. *Acta Metall*, 37(1989): 651–661.
19. K. G. Dassios. *J Comp Mater* 49(2015): 65–74.
20. M. Sutcu. *J Mater Sci* 23(1988): 928–933.
21. K. G. Dassios, V. Kostopoulos and M. Steen. *Acta Mater* 55(2007): 83–92.